Science
AAAS

Cascading Effects of the Loss of Apex Predatory Sharks from a Coastal Ocean
Ransom A. Myers, *et al.*
Science **315**, 1846 (2007);
DOI: 10.1126/science.1138657

Within each ensemble member, emergent model ecotypes typically followed the abundance ranking of their geographically identified real-world counterparts (Fig. 2 and fig. S4): Model ecotypes *m-e1* and *m-e2* ranked first and second (compare these with eMIT9312 and eMED4, respectively), with *m-e3* consistently at lower abundances (compare this with ecotypes eNATL2A and eMIT9313).

There is a simultaneous correspondence between the physiological characteristics of emergent, modeled ecotypes and cultured representatives of the wild population. Each cultured strain of *Prochlorococcus* and the emergent model ecotypes from all 10 ensemble members were characterized by an optimal temperature (T_{opt}) and photon flux (I_{opt}) for growth, the temperature or light intensity at which growth rates are greatest if all other limitations are set aside (fig. S1). Potentially viable *Prochlorococcus* analogs were seeded in the model over wide ranges of optimal temperature and photon fluxes (all circles, Fig. 3), but those that maintained significant abundances along the AMT transect (solid large circles, Fig. 3) were all characterized by $T_{opt} > 15$°C. This is consistent with the observations of *Prochlorococcus* in warmer waters and with the warm T_{opt} of cultured strains (*17*). Our model indicates that the oligotrophic conditions confined *Prochlorococcus* analogs to warmer waters and selected for warm T_{opt}, an emergent "adaptation" driven by other environmental factors. In the cooler waters of the model, nutrients are typically abundant, and so larger phytoplankton, with higher intrinsic maximum growth rates, have an advantage. In the highly oligotrophic (typically warmer) regions, the *Prochlorococcus* analogs' lower half-saturation (consistent with their very small size) is advantageous.

Across the ensemble of 10 integrations, the geographically defined model ecotypes were clustered in optimal temperature and light parameter space (Fig. 3): Model ecotype *m-e1* (red circles) generally occupied the warmest area of parameter space over a broad, upper range of optimal photon fluxes; *m-e2* (blue circles) generally had a lower T_{opt} but a similar range of I_{opt}. This is consistent with their surface-oriented habitats and latitudinal (or temperature) separation. In contrast, *m-e3* (green circles) occupied a wider range of T_{opt} but only in the region of lowest I_{opt}, consistent with its expression of subsurface maxima. Although there were exceptions, the clustering of geographically defined model ecotypes in physiological parameter space indicated that robust ecological controls were operating across the 10 integrations. The physiological characteristics (T_{opt}, I_{opt}) of real-world ecotypes (colored diamonds, Fig. 3) are notably consistent with the grouping of their model counterparts. This correspondence was not imposed, but emerged as a feature of the model solution.

Significantly, there was simultaneous consistency between the geographical habitat, rank abundance, and physiological specialization of the emergent *Prochlorococcus* model ecotypes and their real-world counterparts. These parallels indicate that the stochastic, self-organizing representation of marine ecosystems reflects real-world processes and is suitable for application in ecological and biogeochemical studies. This approach circumvents some of the obstacles facing most current ocean ecosystem models, such as the a priori imposition of low diversity, the prescription of dominant functional types, and the difficulty of specifying the physiological rate coefficients that define them. This function-based approach can naturally evolve to exploit the growing body of genomic and metagenomic data mapping the oceans in terms of genes and their encoded physiological functionality (*25*, *26*). Finally, because the ecosystem structure and function are, by design, emergent and not tightly prescribed, this modeling approach is ideally suited for studies of the relations between marine ecosystems, evolution, biogeochemical cycles, and past and future climate change.

References and Notes

1. D. Tilman, *Ecology* **58**, 338 (1977).
2. R. Margalef, *Perspectives in Ecological Theory* (Univ. of Chicago Press, Chicago, 1968).
3. C. Pedrós-Alió, *Trends Microbiol.* **14**, 257 (2006).
4. S. L. Pimm, J. H. Lawton, *Nature* **268**, 329 (1977).
5. A. Kleidon, H. A. Mooney, *Glob. Change Biol.* **6**, 507 (2000).
6. J. K. Moore, S. Doney, J. Kleyplas, D. Glover, I. Fung, *Deep-Sea Res. II* **49**, 403 (2001).
7. W. W. Gregg, P. Ginoux, P. S. Schopf, N. W. Casey, *Deep-Sea Res. II* **50**, 3143 (2003).
8. E. Litchman, C. A. Klausmeier, J. R. Miller, O. M. Schofield, P. G. Falkowski, *Biogeosciences* **3**, 585 (2006).
9. C. LeQuere *et al.*, *Glob. Change Biol.* **11**, 2016 (2006).
10. T. R. Anderson, *J. Plankton Res.* **27**, 1073 (2005).
11. R. R. Hood *et al.*, *Deep-Sea Res. II* **53**, 459 (2006).
12. P. A. Thompson *et al.*, *Limnol. Oceanogr.* **34**, 1014 (1989).
13. C. Wunsch, P. Heimbach, *Physica D* 10.1016/j.physd.2006.09.040 (2006).
14. Y. Dandonneau, Y. Montel, J. Blanchot, J. Giraudeau, J. Neveux, *Deep-Sea Res. I* **53**, 689 (2006).
15. M. V. Zubkov, M. A. Sleigh, P. H. Burkill, R. J. G. Leakey, *Prog. Oceanogr.* **45**, 369 (2000).
16. H. A. Bouman *et al.*, *Science* **312**, 918 (2006).
17. Z. I. Johnson *et al.*, *Science* **311**, 1737 (2006).
18. L. R. Moore, G. Rocap, S. W. Chisholm, *Nature* **393**, 464 (1998).
19. G. Rocap *et al.*, *Nature* **424**, 1042 (2003).
20. L. R. Moore, S. W. Chisholm, *Limnol. Oceanogr.* **44**, 628 (1999).
21. L. R. Moore, A. F. Post, G. Rocap, S. W. Chisholm, *Limnol. Oceanogr.* **47**, 989 (2002).
22. G. E. Hutchinson, *Am. Nat.* **95**, 137 (1961).
23. R. A. Armstrong, R. McGehee, *Am. Nat.* **115**, 151 (1980).
24. M. W. Lomas, F. Lipschultz, *Limnol. Oceanogr.* **51**, 2453 (2006).
25. J. C. Venter *et al.*, *Science* **304**, 66 (2004).
26. E. F. DeLong *et al.*, *Science* **311**, 496 (2006).
27. S. Bertilsson, O. Berglund, D. M. Karl, S. W. Chisholm, *Limnol. Oceanogr.* **48**, 1721 (2003).

28. Thanks to J. Marshall, R. Williams, P. Falkowski, J. Cullen, and J. Bragg for inspiration and encouragement. Thanks also to M. Coleman, R. Hood, and three anonymous reviewers for stimulating comments on the manuscript; to C. Hill for computing guidance; and to P. Heimbach, C. Wunsch, and the ECCO group for ocean circulation state estimates. We are grateful for funding from the PARADIGM consortium of the National Ocean Partnership Program, NSF (M.J.F., S.D.), NSF, DOE (S.W.C.), and the Gordon and Betty Moore Foundation (S.W.C., M.J.F.). M.J.F. is also grateful for the MIT Global Habitat Longevity Award. We acknowledge the Atlantic Meridional Transect consortium (NER/O/S/2001/00680), which enabled the biogeographical observations first published in (*17*) (AMT contribution no. 107).

Supporting Online Material

www.sciencemag.org/cgi/content/full/315/5820/1843/DC1
Materials and Methods
SOM Text
Figs. S1 to S4
Table S1
References and Notes

7 December 2006; accepted 5 March 2007
10.1126/science.1138544

Cascading Effects of the Loss of Apex Predatory Sharks from a Coastal Ocean

Ransom A. Myers,[1] Julia K. Baum,[1]* Travis D. Shepherd,[1] Sean P. Powers,[2] Charles H. Peterson[3]*

Impacts of chronic overfishing are evident in population depletions worldwide, yet indirect ecosystem effects induced by predator removal from oceanic food webs remain unpredictable. As abundances of all 11 great sharks that consume other elasmobranchs (rays, skates, and small sharks) fell over the past 35 years, 12 of 14 of these prey species increased in coastal northwest Atlantic ecosystems. Effects of this community restructuring have cascaded downward from the cownose ray, whose enhanced predation on its bay scallop prey was sufficient to terminate a century-long scallop fishery. Analogous top-down effects may be a predictable consequence of eliminating entire functional groups of predators.

Ecological impacts of eliminating top predators can be far-reaching (*1*) and include release of mesopredator prey populations from predatory control (*2*) and induction of subsequent cascades of indirect trophic interactions (*3*–*5*). In the oceans, fishing has dispropor-

tionately reduced abundances of apex predators (*6*, *7*), eliciting concern about their conservation and the indirect effects that might ensue from their removal. Despite a rich ecological literature on trophic cascades, consequences of removing oceanic apex predators remain uncertain (*8*–*11*). Although some have argued that in complex marine food webs with many interacting species top-down effects may attenuate (*10*, *11*), fundamental constraints on studying oceanic food webs and apex predators may alternatively hinder detection of such effects. We met this challenge by using a unique compilation of time series data and predator exclusion experiments to investigate ecosystem consequences of functionally eliminating apex predatory sharks.

Exploitation of large (>2 m) sharks has intensified worldwide in recent decades, driven by an upsurge in demand for shark fins and meat (*12*) and in bycatch in many fisheries. Data to assess direct impacts of exploitation on the great sharks are limited but consistently indicate that they have been driven to low levels (*12*–*14*). Whether functional elimination of great sharks also induces indirect ecosystem effects, however, is an open question (*14*).

We hypothesized that weakened top-down control by all elasmobranch-consuming sharks could increase abundances of their elasmobranch prey (rays, skates, and small sharks) and that the enhanced predation by these mesopredators might cascade to lower trophic levels. Because mesopredatory elasmobranchs are relatively large, even as juveniles, and are thus consumed almost exclusively by great sharks (*15*), we inferred that these prey would be the most likely affected. Moreover, interannual variability in elasmobranch populations is minimal because of their low reproductive rates, such that changes effected by predator removal should be detectable in time series data. We tested these hypotheses for 1970–2005 on the United States' eastern seaboard between Cape Cod, Massachusetts (41.5°N) and Cape Canaveral, Florida (28°N).

For each elasmobranch, we modeled population trends in each of several data sets and also in a meta-analysis to yield synthetic estimates of rates of change (*15*). We first assembled all available species-specific data from scientific research surveys that began before 1990 and used standardized methodology. Seventeen surveys, which together cover the eastern U.S. coast (fig. S1), met these criteria (tables S2 and S3; mean time span = 28 years). Trends in relative abundance of each elasmobranch were estimated by fitting generalized linear models (GLMs, table S4) to each survey in which the species appeared in at least 3 years. Because not all great sharks were sampled in surveys and because the U.S. pelagic longline fishery covers a much greater proportion of the sharks' northwest Atlantic ranges, trends for these species also were estimated from this fishery's observer and logbook data [by fitting generalized linear mixed models and GLMs, respectively (*15*)].

The eastern seaboard's longest continuous shark-targeted survey (UNC), conducted annually since 1972 off North Carolina, demonstrates sufficiently large declines in great sharks to imply their likely functional elimination. Declines in seven species range from 87% for sandbar sharks (*Carcharhinus plumbeus*); 93% for blacktip sharks (*C. limbatus*); up to 97% for tiger sharks (*Galeocerdo cuvier*); 98% for scalloped hammerheads (*Sphyrna lewini*); and 99% or more for bull (*C. leucas*), dusky (*C. obscurus*), and smooth hammerhead (*S. zygaena*) sharks (Fig. 1 and table S5). Because this survey is

[1]Department of Biology, Dalhousie University, 1355 Oxford Street, Halifax, NS B3H 4J1, Canada. [2]Department of Marine Sciences, University of South Alabama, and Dauphin Island Sea Lab, 101 Bienville Boulevard, Dauphin Island, AL 36528, USA. [3]Institute of Marine Sciences, University of North Carolina (UNC) at Chapel Hill, Morehead City, NC 28557, USA.

*To whom correspondence should be addressed. E-mail: baum@mscs.dal.ca (J.K.B.); cpeters@email.unc.edu (C.H.P.)

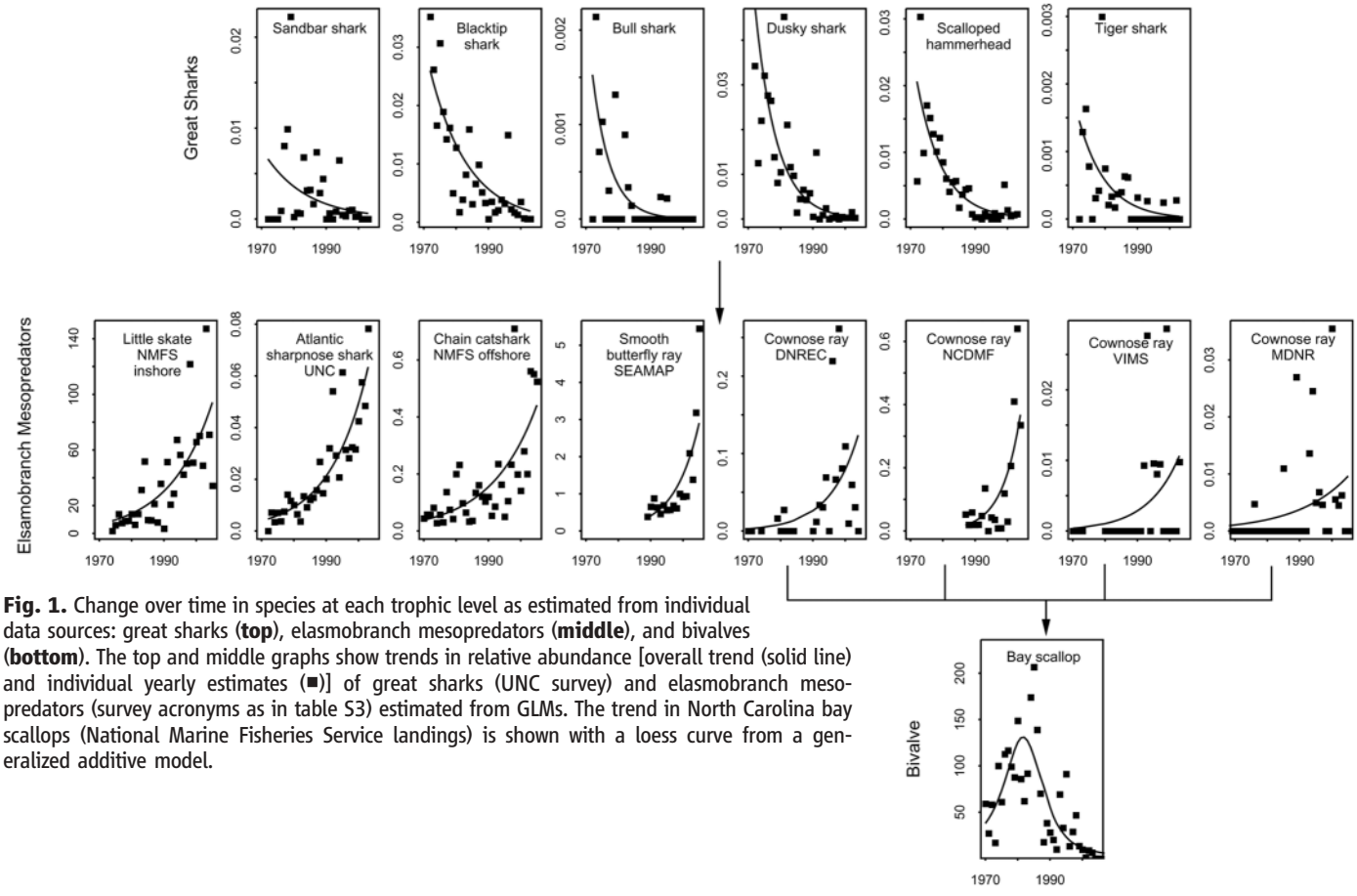

Fig. 1. Change over time in species at each trophic level as estimated from individual data sources: great sharks (**top**), elasmobranch mesopredators (**middle**), and bivalves (**bottom**). The top and middle graphs show trends in relative abundance [overall trend (solid line) and individual yearly estimates (■)] of great sharks (UNC survey) and elasmobranch mesopredators (survey acronyms as in table S3) estimated from GLMs. The trend in North Carolina bay scallops (National Marine Fisheries Service landings) is shown with a loess curve from a generalized additive model.

situated where it intercepts sharks on their seasonal migrations, these trends in abundance may be indicative of coastwide population changes. The UNC survey also showed the loss of the largest individuals, with declines in mean lengths of blacktip, bull, dusky, sandbar, and tiger sharks of 17 to 47% (fig. S3), suggesting that overexploitation has left few mature individuals in these populations. The remaining four elasmobranch-consuming great sharks were caught too rarely to detect trends from this survey. Two of those, great white (*Carcharodon carcharias*) and sand tiger (*Carcharias taurus*) sharks, were each caught only once and early in the UNC survey (in 1974 and 1978, respectively). The only survey that has caught enough sand tigers to note a trend targets sharks in Chesapeake Bay and suggests a decline of over 99% between 1974 and 2004 (*15*, *16*).

Consistent with the UNC survey, all but one of the other six significant survey trends indicate decreasing great shark abundances (table S5). The only significant increase is for juvenile hammerheads from a single survey and consequently may reflect recently increased survival after losses of their only predators, larger apex predatory sharks. Accordingly, meta-analytic results portray a consistent pattern of declines in great sharks (Fig. 2A).

Fisheries data from the past 2 decades help confirm losses of elasmobranch-consuming great sharks (Fig. 2A). Logbook data show declines between 1986 and 2000 ranging from 40% in makos [predominantly shortfin mako (*Isurus oxyrinchus*)] to 89% in hammerheads [scalloped, great (*S. mokarran*), and smooth] (*13*) (table S5). Trend estimates from observer data collected between 1992 and 2005 differ from logbook data for tiger sharks (after a decline, this species may have recently increased) but are concordant for all other species: Makos declined moderately (38%), whereas large coastals (genus *Carcharhinus*, including dusky, sandbar, blacktip, and bull) and hammerheads declined by 67% and 76%, respectively (table S5).

Concurrent with reductions in great sharks, their mesopredatory elasmobranch prey have increased along the eastern seaboard. This group of 14 rays, skates, and small sharks is taxonomically diverse (seven families) and includes demersal and pelagic species from estuaries and the inshore coast to the continental shelf and slope. Individual surveys indicate that little skate (*Leucoraja erinacea*), Atlantic sharpnose shark (*Rhizoprionodon terraenovae*), chain catshark (*Scyliorhinus retifer*), and smooth butterfly ray (*Gymnura altavela*) populations may have each increased by about an order of magnitude (Fig. 1). Overall, meta-analyses of research survey data reveal increases over the past 16 to 35 years for 12 of the species, with estimated mean instantaneous rates of increase ranging from 0.012 for bullnose eagle ray (*Myliobatis freminvillii*) to 0.228 for smooth butterfly ray (Fig. 2B).

Most conspicuous (*17*) among the increasing mesopredators is the cownose ray (*Rhinoptera bonasus*). Six of seven surveys covering the U.S. Atlantic population's range (southeast Florida to Raritan Bay, New Jersey, with recent expansion to Long Island, New York) show significant increases (Fig. 1 and table S5). Together, these rates of change (mean = 0.087, 95% confidence interval 0.021 to 0.127) (Fig. 2B) indicate an order-of-magnitude increase in cownose rays coastwide since the mid-1970s and, when combined with earlier population estimates from aerial surveys in Chesapeake Bay (*18*), suggest that there may now be over 40 million rays in the population. When considered with its known late maturity and low fecundity, this high population growth rate would make the cownose ray anomalous among fishes in its combination of life-history traits (*15*). Only if its natural mortality rate were substantially greater than at present would the life history conform, implying that higher predation by great sharks prevailed in the past and possible reduction in bycatch is insufficient to explain the ascent of this ray.

Collectively, the hyperabundant cownose ray population consumes a large quantity of bivalves, implying a high potential for trophic cascades. Cownose rays migrate southward in autumn from northerly estuaries to overwinter-

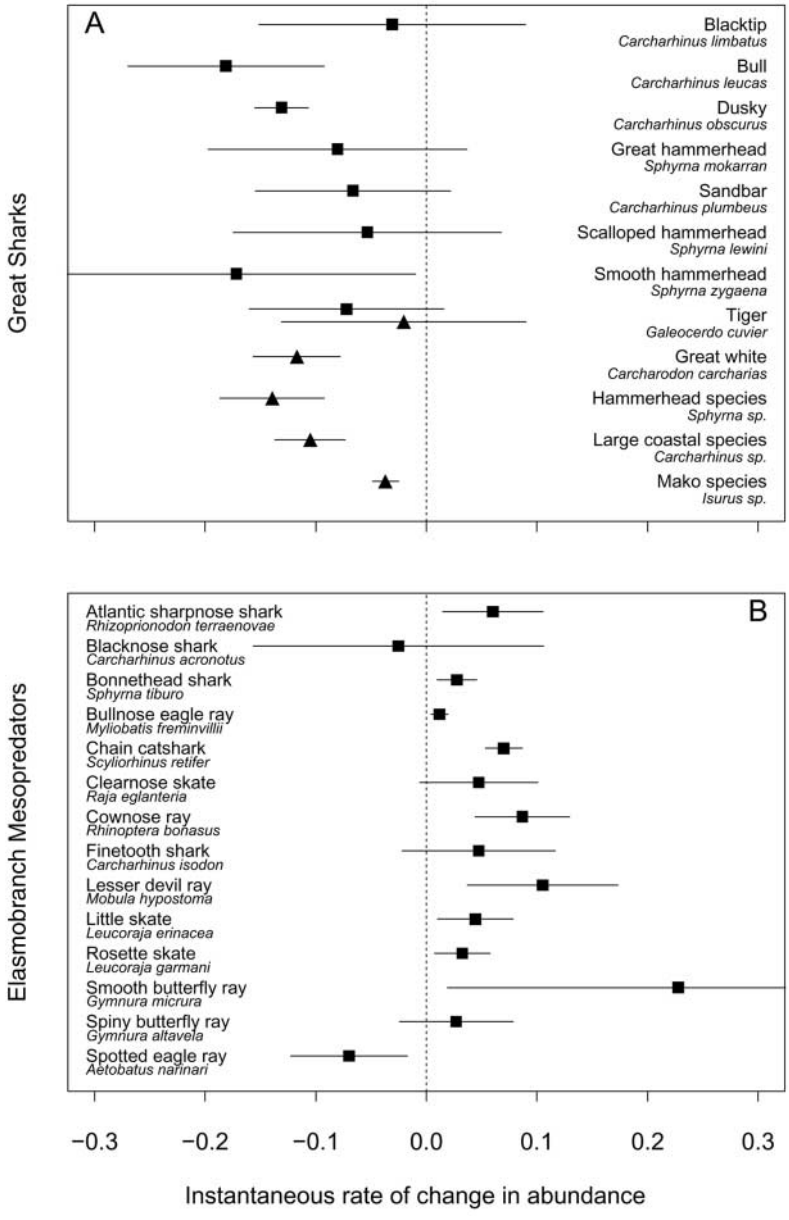

Fig. 2. Instantaneous rates of change in relative abundance (±95% confidence intervals) for (**A**) great sharks and (**B**) elasmobranch mesopredators, as estimated by random-effects meta-analyses of research survey (■) and fisheries (▲) data.

ing grounds on the Florida shelf (*19*), often entering bays and sounds en route. Their diet consists largely of bay scallops (*Argopecten irradians*), soft-shell clams (*Mya arenaria*), hard clams (*Mercenaria mercenaria*), oysters (*Crassostrea virginica*), and several smaller, noncommercial bivalves (*18*, *20*). Annual bivalve demand within the Chesapeake Bay, based on our abundance estimate, individual daily consumption rates of ~210 g shell-free wet weight (*15*), and 100-day occupancy each year, may approach 840,000 metric tons. In comparison, the 2003 commercial bivalve harvest in Virginia and Maryland totaled only 300 metric tons, substantially lower than historic landings (*15*).

A second link in an apparent trophic cascade has emerged over the past 2 decades as the cownose ray population grew coastwide (Figs. 1 and 3). Field sampling in 1983 and 1984 before and after ray presence during late-summer migration showed no impacts of ray predation on bay scallops (Fig. 3A) (*21*). Analogous recent sampling, confirmed by controlled ray-exclusion experiments using stockades, demonstrates that since 1996 migrating cownose rays have caused almost complete scallop mortality by early fall (Fig. 3A) (*22*) at every site with initial adult scallop densities above a threshold for intensive ray foraging (~2 m^{-2}, Fig. 3, B and C). Bay scallop abundance declined much less inside cownose ray exclosures than on unprotected grounds (Fig. 3A) and, in the absence of scallop emigration, numbers inside stockades would probably have remained nearly constant (*22*). Unlike the fishery harvest, which occurs after, ray predation occurs before spawning of this annual species (*23*). By 2004, ray predation had terminated North Carolina's century-old bay scallop fishery because too few scallops survived into fall to sustain fishing and a consequent Allee effect (apparently induced at adult densities below ~1 to 2 m^{-2}) limited reproductive success (*23*). The fishery has remained closed through 2007 (Fig. 1) because of low recruitment and continued ray predation on any high-density patch of scallops. Having depleted the more readily targeted epibiotic bay scallops, it is reasonable to expect future expansion of cownose ray foraging on infaunal bivalves, with associated uprooting of seagrass and thus loss of nursery habitat (*20*, *24*).

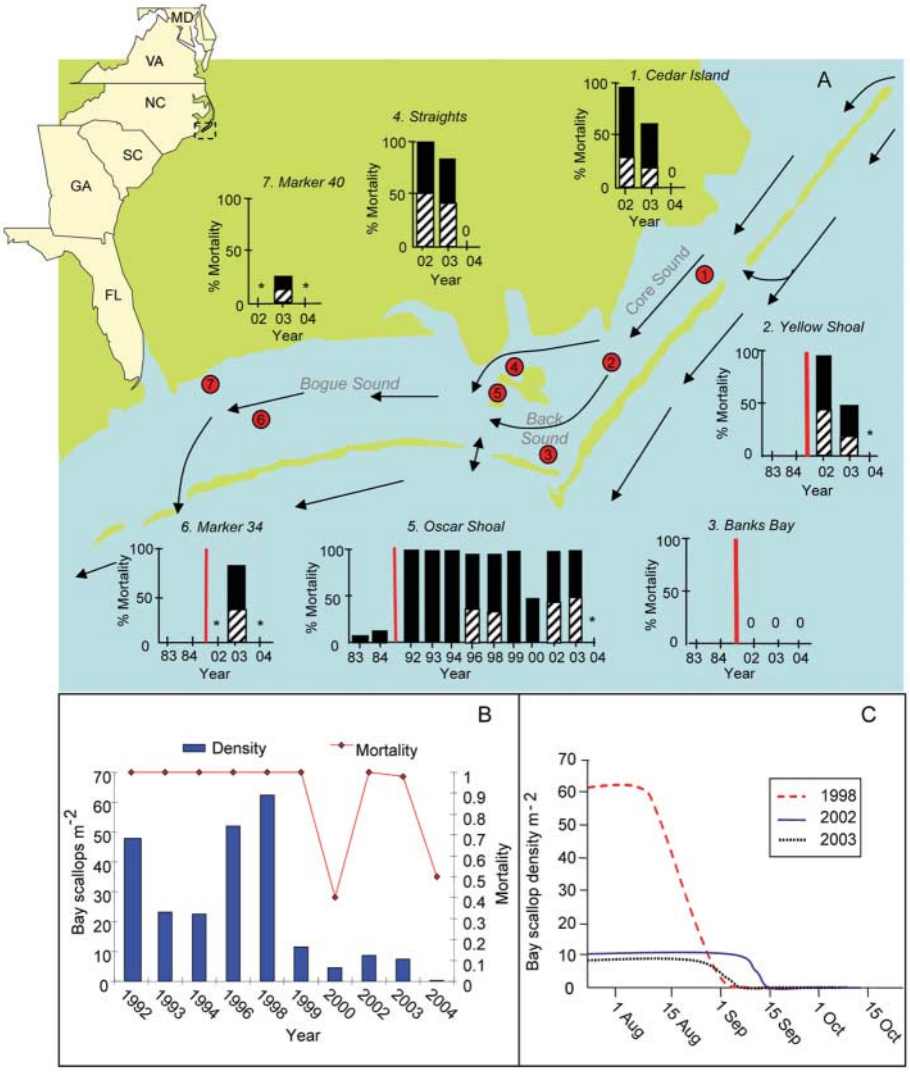

Fig. 3. (**A**) Map of southeastern United States indicating the study location (inset) and North Carolina bay scallop monitoring sites. Total mortality (black bars) compares August (pre–cownose ray migration) to late September and October (postmigration) densities. Low scallop densities before ray migration are indicated by asterisks (<1 to 2 m^{-2}) or zeroes (0 m^{-2}). Hatched bars represent mortality within experimental stockades that exclude rays (performed in a subset of years). Scallops were free to emigrate from stockades. Arrows denote direction of ray migration. (**B**) Mean scallop density measured in midsummer and mortality from early summer to early fall at Oscar Shoal for 10 years. (**C**) Scallop density trends at Oscar Shoal, based on 12 weekly surveys in 1998 and 8 in 2002 and 2003.

Increased predation by cownose rays also may now inhibit recovery of hard clams, soft-shell clams, and oysters (*17*), compounding the effects of overexploitation, disease, habitat destruction, and pollution, which have depressed these species (*7*). Landings data for these bivalves and bay scallops from within the cownose ray's range show them falling without substantial recovery (fig. S2) as the rays increased, despite active shellfish enhancement and habitat restoration. In contrast, areas beyond the ray's northernmost limit show examples of stable or increasing bivalve landings (fig. S2).

Analogous elasmobranch community inversions and trophic cascades are probably occurring in other coastal oceans. Studies in the northeast Atlantic Ocean have shown increasing abundances of several mesopredatory elasmobranchs despite substantial exploitation (*25*, *26*). In Japan's Ariake Sound in the northwest Pacific Ocean, where exploitation of apex predatory sharks is probably intense, wild stocks and cultured populations of multiple shellfish species are now decimated annually by expanding numbers of another elasmobranch mesopredator, the longheaded eagle ray (*Aetobatus flagellum*) (*27*). Many other prey depletions may be going unrecognized because little monitoring and research exists for noncommercial marine species.

Our study provides evidence for an oceanic ecosystem transformation that is most parsimoniously explained by the functional elimination of apex predators, the great sharks, instead of assuming numerous coincidental increases in their mesopredatory prey. Consequences of this region-wide proliferation of rays, skates, and smaller sharks have cascaded down the food web through cownose rays to bay scallops and possibly other bivalves. This cascade potentially could extend to seagrass habitat, exacerbating stresses on already highly degraded coastal

benthic systems. Thus, like the classic killer whale–sea otter–urchin–kelp trophic cascade (*5*), eliminating great sharks carries risks of broader ecosystem degradation. Prevailing theory suggests that community-level trophic cascades arise only in simple food webs lacking functional redundancy (*4*, *10*), but we propose that top-down effects must be widely expected whenever entire functional groups of predators are depressed, as can occur with industrial fisheries. Illuminating the operation of indirect species interactions within marine and other environments brightens the future for development of what is now so widely sought, ecosystem-based management to achieve sustainability of natural living resources.

References and Notes

1. J. E. Duffy, *Oikos* **99**, 201 (2002).
2. K. R. Crooks, M. E. Soulé, *Nature* **400**, 563 (1999).
3. R. T. Paine, *J. Anim. Ecol.* **49**, 667 (1980).
4. M. L. Pace, J. G. Cole, S. R. Carpenter, J. F. Kitchell, *Trends Ecol. Evol.* **14**, 483 (1999).
5. J. A. Estes, M. T. Tinker, T. M. Williams, D. F. Doak, *Science* **282**, 473 (1998).
6. D. Pauly, V. Christensen, J. Dalsgaard, R. Froese, F. Torres Jr., *Science* **279**, 860 (1998).
7. J. B. C. Jackson *et al.*, *Science* **293**, 629 (2001).
8. J. Bascompte, C. J. Melián, E. Sala, *Proc. Natl. Acad. Sci. U.S.A.* **102**, 5443 (2005).
9. K. T. Frank, B. Petrie, J. S. Choi, W. C. Leggett, *Science* **308**, 1621 (2005).
10. D. R. Strong, *Ecology* **73**, 747 (1992).
11. S. Jennings, M. J. Kaiser, *Adv. Mar. Biol.* **34**, 201 (1998).
12. S. L. Fowler *et al.*, Eds., *Sharks, Rays and Chimaeras: The Status of the Chondrichthyan Fishes* (Shark Specialist Group, Species Survival Commission, World Conservation Union, Cambridge, 2005).
13. J. K. Baum *et al.*, *Science* **299**, 389 (2003).
14. J. D. Stevens, R. Bonfil, N. K. Dulvy, P. A. Walker, *ICES J. Mar. Sci.* **57**, 476 (2000).
15. Species information and detailed methods are available on *Science* Online.
16. D. H. Ha, thesis, College of William and Mary, Gloucester Point, VA (2006).
17. D. A. Fahrenthold, *Washington Post*, www.washingtonpost.com/wp-dyn/articles/A29969-2004Aug24.html (25 August 2004).
18. R. A. Blaylock, *Estuaries* **16**, 255 (1993).
19. D. S. Grusha, thesis, College of William and Mary, Gloucester Point, VA (2005).
20. J. W. Smith, J. V. Merriner, *Estuaries* **8**, 305 (1985).
21. C. H. Peterson, H. C. Summerson, S. R. Fegley, R. C. Prescott, *J. Exp. Mar. Biol. Ecol.* **127**, 121 (1989).
22. C. H. Peterson, F. J. Fodrie, H. C. Summerson, S. P. Powers, *Oecologia* **129**, 349 (2001).
23. C. H. Peterson, H. C. Summerson, R. A. Luettich Jr., *Mar. Ecol. Prog. Ser.* **132**, 93 (1996).
24. R. J. Orth, *Chesapeake Sci.* **16**, 205 (1975).
25. N. K. Dulvy, J. D. Metcalfe, J. Glanville, M. G. Pawson, J. D. Reynolds, *Conserv. Biol.* **14**, 283 (2000).
26. S. I. Rogers, J. R. Ellis, *ICES J. Mar. Sci.* **57**, 866 (2000).
27. A. Yamaguchi, I. Kawahara, S. Ito, *Environ. Biol. Fish.* **74**, 229 (2005).

28. We thank J. Boylan, J. Collie, E. Durell, D. Gaskill, J. Hoey, W. Hogarth, D. Kahn, J. Kraeuter, R. Lipcius, M. McDuff, P. Rago, D. Ricard, R. Seitz, D. Simpson, F. Schwartz, J. Smith, G. Ulrich, K. West, and the North Carolina Division of Marine Fisheries (NCDMF) for sharing data. North Carolina biological data were provided at the authors' request by the NCDMF. Analyses of these data and conclusions drawn there from are those of the authors and do not necessarily represent the views of NCDMF. We also thank D. Gaskill for assistance conducting the field research and the UNC Institute of Marine Sciences for providing support to conduct the longline shark survey. V. Garcia, J. Hoenig, H. Lotze, L. Lucifora, A. Sugden, J. Valentine, B. Worm, and the referees provided helpful comments on the manuscript. We acknowledge funding from Pew Institute for Ocean Science, Sloan Census of Marine Life, Natural Sciences and Engineering Research Council of Canada, Killam Trusts, NC Fisheries Resource Grants Program, NC Sea Grant, and NSF.

Supporting Online Material

www.sciencemag.org/cgi/content/full/315/5820/1846/DC1
Materials and Methods
SOM Text
Figs. S1 to S3
Tables S1 to S5

11 December 2006; accepted 5 March 2007
10.1126/science.1138657

Protein Composition of Catalytically Active Human Telomerase from Immortal Cells

Scott B. Cohen,[1] Mark E. Graham,[2] George O. Lovrecz,[3] Nicolai Bache,[4] Phillip J. Robinson,[2] Roger R. Reddel[1]*

Telomerase is a ribonucleoprotein enzyme complex that adds 5′-TTAGGG-3′ repeats onto the ends of human chromosomes, providing a telomere maintenance mechanism for ~90% of human cancers. We have purified human telomerase ~10^8-fold, with the final elution dependent on the enzyme's ability to catalyze nucleotide addition onto a DNA oligonucleotide of telomeric sequence, thereby providing specificity for catalytically active telomerase. Mass spectrometric sequencing of the protein components and molecular size determination indicated an enzyme composition of two molecules each of telomerase reverse transcriptase, telomerase RNA, and dyskerin.

Telomeres, repetitive nucleoprotein structures at the ends of linear chromosomes (*1*), shorten during each cycle of cell division (*2*), providing a counting mechanism to limit the number of times a cell can divide (*3*). Many cancer cells escape limits on proliferation by activating the ribonucleoprotein enzyme telomerase to catalyze the synthesis of telomeric repeats (*4*). The protein component, human telomerase reverse transcriptase (hTERT), contains conserved catalytic reverse transcriptase motifs (*5*, *6*), and the human telomerase RNA component (hTR) (*7*) directs the addition of deoxynucleotide triphosphates (dNTPs) by means of an internal template complementary to the telomeric repeat sequence TTAGGG.

Telomerase has previously been purified only from the ciliate *Euplotes aediculatus* as a complex of TERT, RNA, and associated protein p43 (*8*). At least 32 distinct proteins have been proposed to associate with human telomerase (table S1). Size measurements of human telomerase have indicated a complex larger than expected for a composition of one hTERT (127 kD) and one hTR (153 kD) (*9*, *10*) but smaller than the sum of all proposed protein associations (~2.6 MD). Nonetheless, the precise composition of the active enzyme complex within the cell has remained undefined.

We measured the size of the active human telomerase complex in a panel of immortal cell lines (MCF-7, A2182, HCT-116, TE-85, HT-1080, and HEK-293, derived from cancers of the breast, lung, colon, bone, and connective tissue, and from embryonic kidney cells, respectively). Quantification of telomerase was performed with a direct (non–polymerase chain reaction) primer-extension activity assay (fig. S1). Whole-cell lysates (*11*) from all cell lines exhibited a similar sedimentation profile, with ≥60% of total activity eluting in fractions 9 and 10 (Fig. 1, A to C). Thyroglobulin (669 kD) peaked in fraction 9 (Fig. 1B), indicating that telomerase exists as an enzyme complex of ~650 to 670 kD.

We developed a purification scheme that achieved ~10^8-fold enrichment of active telomerase in three steps (*11*). The first step was immunoaffinity purification with a sheep polyclonal antibody generated against the peptide antigen ARPAEEATSLEGALSGTRH (hTERT amino acids 276 to 294). HEK-293 lysate was incu-

[1]Cancer Research Unit, Children's Medical Research Institute, 214 Hawkesbury Road, Westmead NSW 2145, Australia. [2]Cell Signalling Unit, Children's Medical Research Institute, 214 Hawkesbury Road, Westmead NSW 2145, Australia. [3]Fermentation Lab, Commonwealth Scientific and Industrial Research Organisation, Molecular and Health Technologies, 343 Royal Parade, Parkville VIC 3052, Australia. [4]Department of Biochemistry and Molecular Biology, University of Southern Denmark, Campusvej 55, 5230 Odense M, Denmark.

*To whom correspondence should be addressed. E-mail: rreddel@cmri.usyd.edu.au